THE JOURNAL OF PHYSICAL CHEMISTRY B

Article

pubs.acs.org/JPCB

Effects of Salt, Polyethylene Glycol, and Locked Nucleic Acids on the Thermodynamic Stabilities of Consecutive Terminal Adenosine Mismatches in RNA Duplexes

Xiaobo Gu, Mai-Thao Nguyen, Abigail Overacre, Samantha Seaton, and Susan J. Schroeder*

Department of Chemistry and Biochemistry, Department of Microbiology and Plant Biology, University of Oklahoma, 101 Stephenson Parkway, Norman, Oklahoma 73019, United States

Supporting Information

ABSTRACT: Consecutive terminal mismatches add thermodynamic stability to RNA duplexes and occur frequently in microRNA-mRNA interactions. Accurate thermodynamic stabilities of consecutive terminal mismatches contribute to the development of specific, high-affinity siRNA therapeutics. Consecutive terminal adenosine mismatches (TAMS) are studied at different salt concentrations, with polyethylene glycol cosolutes, and with locked nucleic acid (LNA) substitutions. These measurements provide benchmarks for the application of thermodynamic predictions to different physiological or therapeutic conditions. The salt dependence for RNA duplex stability is similar for TAMS, internal loops, and Watson−Crick duplexes. A unified model for predicting the free energy of an RNA duplex with or without loops and mismatches at lower sodium concentrations is presented. The destabilizing effects of PEG 200 are larger for TAMS than internal loops or Watson−Crick duplexes, which may result from different base stacking conformations, dynamics, and water hydration. In contrast, LNA substitutions stabilize internal loops much more than TAMS. Surprisingly, the average per adenosine increase in stability for LNA substitutions in internal loops is −1.82 kcal/mol and only −0.20 kcal/mol for TAMS. The stabilities of TAMS and internal loops with LNA substitutions have similar favorable free energies. Thus, the unfavorable free energy of adenosine internal loops is largely an entropic effect. The favorable stabilities of TAMS result mainly from base stacking. The ability of RNA duplexes to form extended terminal mismatches in the absence of proteins such as argonaute and identifying the enthalpic contributions to terminal mismatch stabilities provide insight into the physical basis of microRNA−mRNA molecular recognition and specificity.

Terminal mismatches occur frequently in microRNA (miRNA)−mRNA (mRNA) interactions that regulate gene expression through RNA silencing pathways.[1] The thermodynamic stability of the miRNA−mRNA duplex is one important factor in the specificity of mRNA recognition and determination of silencing pathways.[2−5] Accurate thermodynamic stabilities of terminal mismatches can improve the prediction of miRNA−mRNA interactions and design of more specific small RNA oligomers for therapeutic applications.[2,6−8] For example, in a study of 16 siRNAs targeting the CXCR4 oncogene,[2] improved thermodynamic parameters that include consecutive terminal mismatch stabilities showed the predicted stabilities of the siRNA−mRNA duplex to be more stable by an average of 1.5 kcal/mol,[6] which is approximately 1 order of magnitude in a binding constant. Adenosines are the most common nucleotide adjacent to the seed region in microRNA,[9] and thus, the terminal adenosine mismatches (TAMs) motif was selected to study the effects of salt, polyethylene glycol (PEG) cosolutes, and locked nucleic acids (LNA) substitutions on the thermodynamic stabilities of terminal mismatches in RNA duplexes. These measurements provide benchmarks for estimating the stabilities of miRNA−mRNA interactions in biologically relevant conditions. In addition, these measurements provide insight into the fundamental physical forces that determine the stabilities of mismatches at the ends of RNA duplexes.

Counterions are critical for nucleic acid folding and function and neutralize the negative charge on the phosphate backbone in RNA and DNA. Polyelectrolyte theory[10,11] demonstrates that salt effects depend on the charge of the ion, the length of the polymer, and the separation distance of the charges on the polymer. Specific structural motifs may bind metal ions and facilitate tertiary structure formation in addition to nonspecific counterion condensation effects that promote secondary and tertiary structure formation.[12−20] In duplex formation of short RNA oligomers, the salt dependence is a result of the differences in the hydration and counterion condensation in the single strand and duplex conformations. In general, the salt dependence on the thermodynamic stabilities of nucleic acid duplexes depends on the log of the concentration of the salt.[11] The effects of salt concentration have been studied on only a few short RNA duplexes in separate studies.[21−23] The standard melt buffer for the thermodynamic parameters for RNA duplex formation is 1 M NaCl for practical reasons considering the short length of model RNA duplexes and the optimal range of melting temperatures. The salt dependence of DNA duplexes has been studied much more thoroughly.[22,24−27] The sequence dependence and possible end effects[28] in the salt dependence of DNA duplex formation remain under debate, and possible end

Received: December 10, 2012
Revised: March 11, 2013
Published: March 12, 2013

effects in RNA duplexes has not been tested. The effects of salt on hairpin formation are less than the effects on duplex formation because duplex formation requires bringing together two negatively charged single strands.[29] The effects of salt concentration for two model RNA hairpins matched well the predictions based on studies of DNA hairpins.[25] Thermodynamic studies of UNCG and GNRA RNA tetraloops show a log−linear relationship between free energy of hairpin formation and salt concentration.[30] Salt effects on the HIV-TAR RNA hairpin and several model RNA hairpins has been studied systematically by single molecule force experiments.[31] Interestingly, the effects of monovalent salt concentration show little effect on the thermodynamic stabilities of GC pairs or the UCU bulge loop in HIV, but a measurable effect on the stabilities of AU pairs and the hairpin loop.[31] Thus, measurements of the salt dependence of terminal and internal mismatches will provide useful benchmarks for estimating the stabilities of miRNA−mRNA and other RNA duplex interactions in biologically relevant buffers.

PEG is a common crowding reagent in molecular biology and can mimic crowded cellular conditions. Small osmolytes, such as ethylene glycol and trimethylamine oxide (TMAO), destabilize RNA secondary structure but may stabilize or destabilize RNA tertiary structure depending on different specific surface interactions.[32] As a result of excluded volume effects, polyethylene glycol can stabilize RNA tertiary structure and increase enzymatic activity while decreasing requirements for magnesium ions in group I introns and hammerhead ribozymes.[33,34] PEG crowding effects can shift RNA conformational equilibria and stabilize telomerase pseudoknots and HIV Tat-Tar dimers over hairpins.[35,36] Different sizes and hydrogen bonding potential of various PEG crowding reagents can regulate telomerase activity by altering the relative stabilities of DNA G-quadruplexes and DNA−RNA hybrid duplexes.[37] PEG affects the stabilities and water hydration of RNA and DNA quadruplexes.[38,39] PEG also stabilizes DNA triplexes but destabilizes DNA three-way junctions.[40]

In nucleic acid secondary structure, the destabilizing effects of PEG 200 on RNA, RNA−DNA, and DNA duplexes can be attributed to changes in hydration, flexibility of the helical structure, and preferential interactions between the PEG 200 cosolute and RNA bases.[41,42] PEG can also destabilize nucleic acid secondary structure by reducing the local ion concentrations in RNA and DNA duplexes and hairpins, although Z-form DNA duplexes are stabilized by PEG at high salt concentrations.[43] The effects of PEG on DNA duplexes have been studied much more extensively than RNA duplexes. Thermodynamic studies on the effects of different molecular weight PEG and different DNA duplex lengths show a wide range of changes in melting temperatures from −0.8 to −15.9 °C.[44] The destabilizing effects of PEG on DNA duplexes can be attributed to changes in water hydration around the duplex and a greatly increased dissociation rate.[45,46] PEG 200 can compete with water and preferentially interact with DNA bases in the single strand conformation.[42] The quantified effect of a solute on a process such as duplex formation, the m-value, for PEG 200 is −0.21 ± 0.01, which is similar to the m-value of diethylene glycol.[42] The m-value for PEG 200 is less than predictions that assume only preferential interactions and thus implies that excluded volume is significant and/or the fraction of exposed PEG surface area is less than 1.[42] Although PEG 200 destabilizes Watson−Crick pairs, Hoogsteen pairs in DNA may be stabilized by PEG 200 due to different base stacking and water hydration.[47] This interesting result leads to the hypothesis that if TAMs continue to stack in an A-form RNA helix, then PEG would be predicted to destabilize the duplex, but if TAMs form Hoogsteen pairs, then PEG may stabilize the TAMs. No measurements have been made of the effects of PEG on RNA duplexes containing internal or terminal mismatches. These results provide insight into how PEG affects the equilibrium of RNA duplex formation, such as miRNA-mRNA interactions.

Locked nucleic acids (LNA) have a methylene O2′−C4′ linker rather than a 2′OH group in the ribose (Figure 1).[48] This

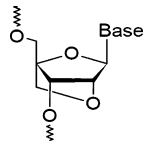

Figure 1. Chemical structure of locked nucleic acid.

fixes the ribose conformation in the C3′ endo form, and preorganizes the nucleic acid for A-form helix formation.[49,50] Oligonucleotides with LNA are effective therapeutics in vitro and in vivo against Hepatitis C,[51−53] *Candida albicans* group I intron splicing,[54] and cancer gene mRNA.[55−58] LNA can reduce off-target effects[59,60] and increase mismatch discrimination.[61−63] Only 2 LNA substitutions on the 3′ end of an siRNA are sufficient to increase oligomer half-life in the cell, increase silencing efficacy, and reduce off-target effects in a mouse tumor model.[58] The tremendous therapeutic applications of LNA have spurred many thermodynamic studies of the sequence and context dependent effects of LNA in DNA, DNA:RNA, and 2′O-methylRNA duplexes.[50,64−67] The thermodynamic stabilities of LNA substitutions in Watson−Crick pairs is the result of increased stacking interactions, reduced ribose entropy, preorganization, increased uptake of sodium ions, and reduced uptake of water.[50,66,67] In 2′O-methyl RNA duplexes, LNA substitutions in single terminal mismatches are energetically favorable while substitutions in internal mismatches are destabilizing.[61] The effects of LNA substitutions on consecutive terminal and internal mismatches in RNA duplexes have not been studied previously. In addition to providing benchmarks for the improved design of LNA therapeutics, comparison of internal and terminal mismatch stabilities provides an estimate of the energetic cost of closing an internal loop. Although internal adenosine mismatches have unfavorable free energies,[68] LNA substitutions make internal loops with adenosines energetically favorable. The measured average per adenosine energetic cost of forming an internal loop versus a terminal mismatch is 1.0 kcal/mol. This suggests that the energetic cost of forming an internal loop is mainly an entropic effect and less affected by changes in base stacking and hydrogen bonding interactions.

METHODS

Oligoribonucleotides were purchased from Dharmacon and deblocked according to the manufacturer's instructions. Greater than 90% purity was confirmed by ^{32}P labeling and denaturing gel electrophoresis. Oligoribonucleotides containing locked nucleic acids were purchased from Eurogentec and required no further deblocking. Purity was confirmed by the manufacturer with mass spectrometry. RNA was dissolved in 1 M or 100 mM NaCl, 10 mM sodium cacodylate, 0.5 mM Na_2EDTA, pH 7

Table 1. Thermodynamic Parameters of Duplex Formation[a]

sequence	conditions	1/T_m plot				melt curve			
salt effects		$-\Delta G°37$ (kcal/mol)	$-\Delta H°$ (kcal/mol)	$-\Delta S°$ (cal/molK)	T_m (°C)[b]	$-\Delta G°37$ (kcal/mol)	$-\Delta H°$ (kcal/mol)	$-\Delta S°$ (cal/molK)	T_m (°C)[b]
5′**AAA**GCGC**AAA**	1 M NaCl[c]	8.94 ± 0.33	57.87 ± 5.35	157.74 ± 16.24	55.5	8.63 ± 0.15	52.14 ± 1.88	140.30 ± 6.01	55.6
	100 mM NaCl	6.98 ± 0.18	44.95 ± 7.74	122.70 ± 24.03	45.7	6.98 ± 0.18	47.89 ± 5.20	131.91 ± 16.34	45.7
	10 mM NaCl	*5.11 ± 0.13*	*38.13 ± 5.95*	*106.47 ± 18.98*	*32.5*	*5.17 ± 0.06*	*45.00 ± 0.85*	*128.41 ± 2.65*	*33.6*
5′**AA**GCGC**AA**	1 M NaCl[c]	8.31 ± 0.40	53.08 ± 24.0	144.35 ± 7.15	53.2	8.19 ± 0.54	51.03 ± 1.76	138.13 ± 5.40	53.0
	100 mM NaCl	6.61 ± 0.11	42.91 ± 1.70	117.04 ± 5.13	43.9	6.79 ± 0.01	47.55 ± 0.42	131.42 ± 1.29	44.4
	10 mM NaCl	3.21 ± 0.15	43.19 ± 3.67	128.90 ± 12.26	20.3	3.43 ± 0.50	37.29 ± 2.07	109.17 ± 6.83	19.4
5′**A**GCGC**A**	1 M NaCl[c]	7.98 ± 0.13	51.70 ± 2.58	140.98 ± 7.92	51.4	7.69 ± 0.12	45.42 ± 1.46	121.65 ± 4.91	51.4
	100 mM NaCl	6.52 ± 0.02	44.59 ± 1.37	122.76 ± 4.40	43.0	6.63 ± 0.12	44.26 ± 4.25	121.32 ± 13.60	43.8
	10 mM NaCl	5.49 ± 0.07	35.51 ± 1.72	96.80 ± 5.72	35.4	5.46 ± 0.12	39.42 ± 4.22	109.49 ± 13.72	35.4
5′CGC**AAA**GCG[g]	1 M NaCl[d]	*4.88*	*45.92*	*132.33*	*31.7*	*5.19*	*30.09*	*80.26*	*32.1*
5′CGC**AA**GCG	1 M NaCl[d]	*5.44*	*48.02*	*137.30*	*35.5*	*5.59*	*40.11*	*111.30*	*36.4*
	100 mM NaCl	4.57 ± 0.13	42.35 ± 2.69	121.80 ± 9.03	29.1	4.62 ± 0.29	44.30 ± 7.85	127.91 ± 26.11	29.8
	10 mM NaCl	2.99 ± 0.33	43.33 ± 5.42	130.06 ± 18.39	18.9	3.16 ± 0.37	40.75 ± 4.84	121.20 ± 16.65	19.0
5′CGC**A**GCG	1 M NaCl[b]	6.09	49.98	141.53	39.6	6.16	47.69	133.39	40.1
	100 mM NaCl	5.33 ± 0.04	53.70 ± 1.65	155.96 ± 5.42	35.0	5.35 ± 0.10	54.31 ± 3.03	157.84 ± 9.90	35.2
	10 mM NaCl	4.12 ± 0.06	45.11 ± 1.820	132.15 ± 4.33	26.7	3.93 ± 0.27	50.92 ± 5.80	151.50 ± 19.25	26.7
5′UUAUCGAUAA[g]	1 M NaCl[e]	9.21	82.3	235.8	50.8	8.9	72.6	205.5	51.2
	100 mM NaCl	6.66 ± 0.03	72.14 ± 2.32	211.12 ± 7.55	41.3	6.75 ± 0.28	75.36 ± 7.65	221.21 ± 24.23	41.5
5′UAUCGAUA	1 M NaCl[e]	7.1	61.8	176.2	44.4	7.2	61.8	176.3	44.6
	100 mM NaCl	5.64 ± 0.03	52.53 ± 1.24	151.18 ± 4.10	36.8	5.48 ± 0.16	62.5 ± 4.21	183.85 ± 13.42	36.0
	10 mM NaCl	3.89 ± 0.26	53.16 ± 3.96	158.83 ± 13.56	26.9	3.59 ± 0.17	58.15 ± 4.70	175.92 ± 15.56	26.3
5′AGCGCU	1 M NaCl[f]	7.8	49.5	134.5	50.6	7.9	50.8	138.5	51.0
	100 mM NaCl	7.24 ± 0.05	44.12 ± 2.12	118.9 ± 6.72	48.4	7.42 ± 0.23	51.69 ± 3.96	142.74 ± 12.11	47.8
	10 mM NaCl[f]	5.5	42.3	118.6	35.7	5.6	46.3	131.3	36.3
5′CGCGCG	1 M NaCl[d]	9.21	54.74	146.77	58.4	9.38	56.93	153.29	58.6
	100 mM NaCl	8.56 ± 0.10	60.43 ± 2.56	167.24 ± 7.96	52.5	8.34 ± 0.16	54.68 ± 1.31	149.41 ± 4.02	52.9
	10 mM NaCl	7.02 ± 0.02	55.95 ± 1.44	157.78 ± 4.60	44.6	7.07 ± 0.06	55.43 ± 4.10	155.94 ± 13.09	45.0
PEG effects									
5′**AAA**GCGC**AAA**	20% PEG200	4.45 ± 0.20	47.73 ± 6.54	139.55 ± 21.55	29.2	4.48 ± 0.14	47.65 ± 2.71	139.21 ± 9.01	29.4
5′**AA**GCGC**AA**	20% PEG200	4.80 ± 0.65	38.11 ± 10.98	107.41 ± 35.13	30.0	4.77 ± 0.16	45.72 ± 1.93	132.03 ± 5.91	30.9
5′**A**GCGC**A**	20% PEG200	6.81 ± 0.38	49.13 ± 8.65	136.42 ± 26.88	44.4	6.72 ± 0.08	45.93 ± 3.79	126.41 ± 12.09	44.2
5′CGC**AAA**GCG	20% PEG200	4.59 ± 0.05	39.46 ± 2.07	112.43 ± 6.84	28.7	4.75 ± 0.21	35.23 ± 5.61	98.30 ± 18.79	29.0
5′CGC**AA**GCG	20% PEG200	4.62 ± 0.09	54.60 ± 2.88	161.13 ± 9.56	31.1	4.68 ± 0.15	52.97 ± 2.94	155.68 ± 9.63	31.3
5′CGC**A**GCG	20% PEG200	5.00 ± 0.07	50.30 ± 2.24	146.04 ± 7.43	32.9	4.99 ± 0.11	53.45 ± 4.30	156.24 ± 14.07	33.1
5′UUAUCGAUAA	20% PEG200	6.94 ± 0.04	62.76 ± 2.46	179.97 ± 7.99	43.4	7.02 ± 0.48	75.25 ± 9.17	220.00 ± 28.54	42.6
5′UAUCGAUA	20% PEG200	5.83 ± 0.03	64.31 ± 2.34	188.57 ± 7.64	37.7	5.85 ± 0.08	63.86 ± 2.62	187.03 ± 8.30	37.9
5′AGCGCU	20% PEG200	6.60 ± 0.16	51.85 ± 5.35	145.9 ± 17.30	42.6	6.57 ± 0.18	53.30 ± 3.43	150.68 ± 11.46	42.3
5′CGCGCG	20% PEG200	8.55 ± 0.16	67.13 ± 4.26	188.86 ± 13.27	50.9	8.23 ± 0.17	57.60 ± 2.00	159.16 ± 6.75	51.4

dx.doi.org/10.1021/jp312154d | J. Phys. Chem. B 2013, 117, 3531−3540

Table 1. continued

sequence	conditions	1/T_m plot				melt curve			
salt effects		$-\Delta G°37$ (kcal/mol)	$-\Delta H°$ (kcal/mol)	$-\Delta S°$ (cal/molK)	T_m (°C)[b]	$-\Delta G°37$ (kcal/mol)	$-\Delta H°$ (kcal/mol)	$-\Delta S°$ (cal/molK)	T_m (°C)[b]
LNA substitutions									
5′$\mathbf{A_LA_LA_L}$GCGC$\mathbf{A_LA_LA_L}$	100 mM NaCl	8.30 ± 0.27	59.71 ± 6.34	165.77 ± 19.78	51.2	8.05 ± 0.36	51.01 ± 11.03	138.51 ± 34.64	52.2
5′$\mathbf{A_LA_L}$GCGC$\mathbf{A_LA_L}$	100 mM NaCl	7.59 ± 0.42	44.78 ± 6.56	119.89 ± 20.31	50.9	7.58 ± 0.43	41.86 ± 9.98	110.51 ± 30.98	51.8
5′$\mathbf{A_L}$GCGC$\mathbf{A_L}$	100 mM NaCl	6.77 ± 0.02	31.77 ± 1.65	80.60 ± 5.30	48.1	7.01 ± 0.50	41.11 ± 2.58	109.94 ± 7.83	47.4
5′CGC$\mathbf{A_LA_LA_L}$GCG	100 mM NaCl	7.75 ± 0.08	56.47 ± 2.71	157.07 ± 8.49	48.8	7.81 ± 0.34	55.85 ± 9.49	154.91 ± 29.56	49.3
5′CGC$\mathbf{A_LA_L}$GCG	100 mM NaCl	8.03 ± 0.10	63.9 ± 3.20	180.12 ± 10.02	48.9	7.9 ± 0.16	56.66 ± 8.31	157.22 ± 26.32	49.7
5′CGC$\mathbf{A_L}$GCG	100 mM NaCl	7.24 ± 0.43	54.65 ± 8.75	152.85 ± 27.26	46.1	7.31 ± 0.61	53.48 ± 7.12	148.89 ± 21.36	46.8
5′CGC$\mathbf{A_L}$GCG	1 M NaCl	8.45 ± 0.13	59.34 ± 2.86	164.1 ± 8.81	52.2	8.19 ± 0.17	51.76 ± 5.43	140.49 ± 17.04	52.8

[a]Melting experiments were done in 10 mM sodium cacodylate, 0.5 mM Na_2EDTA, pH 7.0 buffer with the amount of sodium chloride indicated in column 2. All experiments with polyethylene glycol (PEG) use 1 M NaCl. Sequences and data in italics have differences in enthalpies from van't Hoff plots and curve fitting of 15% or above. Listed errors are standard deviations from reported measurements assuming no correlation of errors in the slope and intercept and are therefore overestimates of this source of error. Estimated errors from all sources are ±10%, ± 10%, and ±2% for $\Delta H°$, $\Delta S°$, and $\Delta G°$, respectively. [b]Melting temperatures are given for total strand concentration of 1×10^{-4} M. [c]Experiments for these terminal mismatches were done in 1 M NaCl after dialysis in 1 mM NaCl and showed no significant difference from previous measurements on undialyzed samples.[6] [d]Values are from ref 68. [e]Values are from ref 74. [f]Values are from ref 6. [g]No 2-state transition was observed for 5′CGCAAAGCG at 100 or 10 mM NaCl and for 5′UUAUCGAUAA at 10 mM NaCl.

Table 2. Effects of Salt, PEG 200, and LNA on Free Energies of Duplex Formation[a]

sequence	$\Delta G°_{duplex}$ (kcal/mol) 1 M NaCl	$\Delta\Delta G°_{duplex}$ (kcal/mol) 100 mM NaCl	$\Delta\Delta G°_{duplex}$ (kcal/mol) 10 mM NaCl	$\Delta\Delta G°_{duplex}$ (kcal/mol) 20%PEG200	$\Delta\Delta G°_{duplex}$[b] (kcal/mol) LNA
TAMS					
5′**AAA**GCGC**AAA**	−8.94	+1.96	+3.83	+4.49	−1.32
5′**AA**GCGC**AA**	−8.31	+1.70	+5.10	+3.51	−0.98
5′**A**GCGC**A**	−7.98	+1.46	+2.49	+1.18	−0.25
average change per phosphate, nucleotide, or LNA substitution		+0.25 ± 0.04	+0.55 ± 0.15	+0.36 ± 0.14	−0.20 ± 0.06
internal loops					
5′CGC**AAA**GCG	−4.88			+0.29	
5′CGC**AA**GCG	−5.44	+0.87	+2.45	+0.82	−3.46
5′CGC**A**GCG	−6.09	+0.76	+1.97	+1.09	−1.91
average change per phosphate, nucleotide, or LNA substitution		+0.12 ± 0.00	+0.34 ± 0.01	+0.10 ± 0.06	−1.82 ± 0.13
Watson−Crick duplex					
5′UUAUCGAUAA	−9.21	+2.55		+2.27	
5′UAUCGAUA	−7.10	+1.46	+3.21	+1.27	
5′AGCGCU	−7.80	+0.56	+2.30	+1.20	
5′CGCGCG	−9.21	+0.65	+2.19	+0.66	
average change per phosphate, nucleotide, or LNA substitution		+0.18 ± 0.08	+0.45 ± 0.01	+0.17 ± 0.09	

[a]$\Delta\Delta G$ values are the difference between the same sequence measured in 1 M NaCl and a different condition from the van't Hoff plot values in Table 1 at 37 °C. A positive $\Delta\Delta G$ value indicates a destabilizing effect, and a negative $\Delta\Delta G$ value indicates a stabilizing effect. The $\Delta\Delta G$ value can be divided by the number of phosphates, LNA substitutions, or nucleotides in the duplex to generate $\Delta\Delta G$ per phosphate, per LNA substitution, or per nucleotide value. Then the average of these normalized values are reported for each RNA motif group. The sequence 5′CGCAAAGCG could not be studied in 100 mM or 10 mM NaCl, which prevents some comparisons. [b]$\Delta\Delta G$ values are calculated for duplexes measured in 100 mM NaCl with and without LNA.

melting buffer. For RNA used in salt dependence studies, the stock RNA was dialyzed in 1 mM NaCl, 10 mM sodium cacodylate, 0.5 mM Na_2EDTA, pH 7 buffer and then the NaCl concentration was adjusted to the appropriate concentration. No significant differences were observed in the thermodynamic parameters from dialyzed and nondialyzed samples with 1 M or 100 mM NaCl final buffer concentration. Buffers with varying percentage by volume polyethylene glycols and 1 M NaCl, 10 mM sodium cacodylate, 0.5 mM Na_2EDTA, pH 7 were also used for studies on crowding conditions.

Oligomer concentration was determined at 260 or 280 nm absorbance at 80 °C.[69] Melting curves were measured at 260 or 280 nm on a Beckman DU800 spectrometer with a modified microT_m cell holder and a heating rate of 1 °C/min. The melting curves were fit to a two-state model with sloping baselines[70] as analyzed with the Meltwin program.[71] Thermodynamic parameters were obtained by averaging values of individual fits to curves and by fitting plots of inverse melting temperature (T_M^{-1}) versus the natural log of the total strand concentration (C_T) to the equation:

dx.doi.org/10.1021/jp312154d | J. Phys. Chem. B 2013, 117, 3531−3540

$$T_M^{-1} = (R/\Delta H^\circ)\ln(C_T) + \Delta S^\circ/\Delta H^\circ \quad (1)$$

where R is the gas constant.[72] Data analysis was done with Excel software.

RESULTS AND DISCUSSION

Table 1 shows the optical melting data for a series of terminal adenosines mismatches (TAMS) and internal loops containing adenosines in 1 M, 100 mM, or 10 mM NaCl, with locked nucleic acid substitutions, or with PEG 200. Four Watson−Crick duplexes are studied in the different salt and PEG 200 conditions in order to compare mismatches with standard A-form RNA helices. The data analyses for both the van't Hoff plot (eq 1) and the curve fitting are shown in order to estimate the validity of the two-state assumption in the calculations of the thermodynamic parameters. Melting experiments with debatable two-state behavior are shown in italics. Some sequences could not be studied at lower salt concentrations because the duplex became too unstable as evidenced by low melting temperatures that precluded fitting the lower baseline, clearly nontwo state behavior, or no observable transition. The duplexes with LNA substitutions were studied at 100 mM NaCl because the melting temperatures are too high in 1 M NaCl to measure accurately and to fit an upper baseline. The temperature accuracy of the Beckman DU 800 UV−vis spectrometer is within ±0.5 °C up to only 60 °C. Only one duplex with LNA, 5′ CGCA$_L$GCG, was studied in 1 M NaCl.

The Effects of Salt Are Similar and Predictable for TAMS, Internal Loops, and A-Form RNA Duplexes. Table 2 columns 3 and 4 show the changes in free energy of duplex formation when the salt condition is reduced from 1 M to 100 mM or 10 mM NaCl. The free energy change depends on the length of the duplex and the number of phosphates, which is predicted by polyelectrolyte theory[10,11] and comparisons to salt effects in DNA duplexes.[24] The average free energy changes per phosphate for duplexes with TAMS or internal loops and Watson−Crick A-form duplexes are 0.25 kcal/mol, 0.12 kcal/mol, and 0.18 kcal/mol, respectively in 100 mM NaCl, and 0.55 kcal/mol, 0.34 kcal/mol, and 0.45 kcal/mol respectively in 10 mM NaCl. The free energy changes for TAMS, internal loops, and A-form duplexes are within experimental error for optical melting experiments. The changes in free energies in 10 mM NaCl are approximately twice the change in free energies in 100 mM NaCl. There is a slightly larger effect for TAMS in 10 mM NaCl than either internal loops or A-form duplexes, but the error is also larger and there are too few measurements to be a significant difference.

Previous measurements of RNA duplexes in 100 mM NaCl[22,23] and 10 mM NaCl[21] can be included in the data set to develop prediction rules for salt effects in RNA. The thermodynamic data for 6 nonself-complementary Watson−Crick duplexes in 100 mM NaCl is compared to predicted free energies in 1 M NaCl using the NN-HB nearest neighbor rules.[73] These data points have a slightly larger error because the sequences contain many consecutive AU pairs, which sometimes display non-nearest neighbor effects in predicted free energies.[74] The free energy changes for Watson−Crick duplexes in 10 mM NaCl and 1 M NaCl is back-calculated from data presented in[21] and includes duplexes with an additional 5′ or 3′ phosphate. All together with the data in Table 1, the data set contains 39 data points, 15 in 10 mM NaCl and 24 in 100 mM NaCl. The overall average free energy change per phosphate per order of magnitude in salt concentration is 0.29 ± 0.11 kcal/mol. This leads to the following prediction rule:

$$\Delta G^\circ(\text{low salt}) = \Delta G^\circ(\text{high salt}) + 0.29 \times(\text{no. phosphates}) \times[\log_{10}(\text{mM high salt}) - \log_{10}(\text{mM low salt})] \quad (2)$$

The fit of experimental and predicted free energies for duplexes in 100 and 10 mM NaCl is shown in Figure 2. The R^2 value is 0.892 for a linear fit of the data in Figure 2. The data points from predicted duplex free energies in 1 M NaCl are shown in green. The complete data set is provided in the Supporting Information Table S1. All of the RNA duplexes are too short to evaluate potential end effects. Fitting the data with or without sequences containing mismatches gave equivalent statistics. This suggests that nonspecific salt stabilization effects from sodium chloride are not sensitive to local perturbations in A-form RNA, unlike site-specific stabilizing effects of magnesium ions.[14,23]

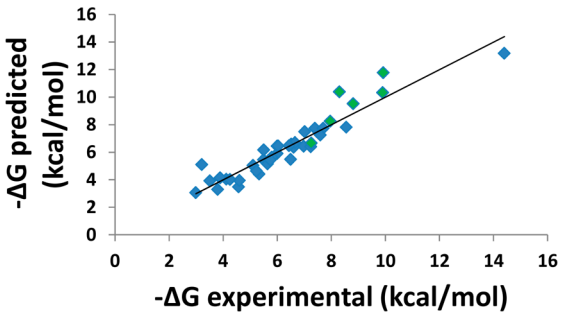

Figure 2. Fit of experimental free energies and predicted free energy values for RNA duplexes in 10 or 100 mM NaCl using eq 2. The data set includes measurements in Table 1 as well as previous measurements in refs 21−23. Data points generated using predicted values for the free energy of duplex formation in 1 M NaCl[22,73] are shown in green. The R^2 value for the fit of the line is 0.892.

The form of eq 2 follows the format of rules for predicting stabilities of DNA Watson−Crick duplexes[24] and has a similar slope within experimental error. Predictions using eq 2 or the prediction rule for DNA oligomers give equivalent statistics. This suggests that salt effects are not sensitive to the differences in A-form and B-form nucleic acid duplexes and supports the simplifying assumptions made in Poisson−Boltzmann and Manning theories describing the effects of salt on a linear charged polymer. Equation 2 includes consideration of the number of phosphates in the RNA oligomer, unlike a previous prediction rule for salt effects in RNA duplexes,[22] in order to more closely follow physical models of salt effects on charged polymers with Poisson−Boltzmann or Manning theory. The prediction rule presented by Nakano et al.[22] generates similar statistics within experimental error for the 24 data points in 100 mM NaCl, but makes no predictions for RNA duplexes in 10 mM NaCl. Equation 2 thus presents a useful, unified model for predicting the stabilities of RNA duplexes with or without mismatches and loops at lower salt concentrations.

The Destabilizing Effect of PEG is Larger for TAMS than for Internal Loops. The next column of Table 2 shows the effects of adding 20% PEG 200 on RNA duplex stability. The range of free energy changes for TAMS is 4.49 to 1.18 kcal/mol with an average per nucleotide change of 0.36 ± 0.14

dx.doi.org/10.1021/jp312154d | J. Phys. Chem. B 2013, 117, 3531−3540

Table 3. Effects of Different Molecular Weight PEG on Thermodynamics Stabilities of Terminal Mismatches

sequence	5% PEG (ave.MW)	$-\Delta G^{\circ}$ (kcal/mol)	$-\Delta H^{\circ}$ (kcal/mol)	$-\Delta S^{\circ}$ (cal/molK)	T_m (°C)	concentration ($\times 10^{-6}$ M)
5′**AAAA**GCGC**AAAA**	none	9.01	51.43	136.78	49.30	10.77
	200	8.56	49.57	132.24	46.89	11.19
	400	8.69	50.40	134.48	47.69	11.52
	3350	8.80	51.57	137.88	48.05	11.12
	6000	8.84	53.46	143.84	48.05	11.57
	8000	8.86	52.47	140.60	48.45	11.87
5′**AAA**GCGC**AAA**	none	9.00	50.58	134.07	49.14	10.04
	200	8.61	50.47	134.94	46.83	10.52
	400	8.74	51.58	138.14	47.53	10.87
	3350	8.80	51.73	138.43	47.80	10.63
	6000	8.77	54.09	146.13	47.37	11.39
	8000	8.84	54.61	147.60	47.58	11.03
5′**AA**GCGC**AA**	none[a]	8.56	47.83	126.63	45.24	6.97
	200	8.38	44.96	117.94	44.10	6.37
	400	8.55	48.58	129.07	44.87	6.65
	3350	8.22	43.42	113.47	43.90	7.41
	6000	8.61	52.51	141.54	44.75	6.81
	8000	8.20	45.65	120.76	43.01	6.82
5′**A**GCGC**A**	none	7.78	47.88	129.28	40.62	8.07
	200	8.22	50.04	134.86	43.56	8.73
	400	8.54	46.27	121.64	46.62	9.16
	3350	8.31	46.54	123.25	44.67	8.57
	6000	8.31	50.16	134.93	44.16	8.68
	8000	8.34	57.87	159.71	43.38	8.79
5′UUAUCGAUAA	none[b]	8.87	70.14	197.53	44.74	8.95
	200	8.51	72.07	204.94	42.83	8.78
	400	8.62	71.58	203.2	43.57	9.42
	3350	8.68	71.22	201.63	43.83	9.18
	6000	8.71	73.80	209.88	43.65	9.02
	8000	8.73	75.52	215.34	43.80	9.68

[a]Values from ref 6. [b]Values from ref 74.

Table 4. Effects of Different Percentages of PEG200 and PEG8000 on the Thermodynamic Stability of 5′UUAUCGAUAA

%	PEG (ave.MW)	$-\Delta G^{\circ}$ (kcal/mol)	$-\Delta H^{\circ}$ (kcal/mol)	$-\Delta S^{\circ}$ (cal/molK)	T_m (°C)	concentration (1×10^{-6} M)
0	none[a]	9.02	71.88	202.66	45.80	10.97
5	200	8.69	72.97	207.27	44.41	12.02
10	200	8.33	72.86	208.07	42.74	11.59
15	200	7.92	74.13	213.47	40.93	11.80
20	200	7.52	74.74	216.74	39.24	12.02
0	8000	8.73	75.52	215.34	43.80	9.68
5	8000	8.94	75.55	214.76	45.84	14.97
10	8000	8.83	77.17	220.35	45.32	15.73
15	8000	8.71	78.04	223.53	44.78	16.05
20	8000	7.68	71.55	205.93	39.32	92.0

[a]Values from ref 74

kcal/mol. For internal loops, the range of free energy changes is smaller, 0.29 to 1.09 kcal/mol with an average per nucleotide change of 0.1 ± 0.06 kcal/mol. The trend in internal loop stabilities with longer duplexes is opposite in direction compared to TAMS and Watson–Crick pairs. In Watson–Crick RNA duplexes, the range of free energy changes is 2.27 to 0.66 kcal/mol with an average per nucleotide change of 0.17 ± 0.09 kcal/mol. The $\Delta\Delta G^{\circ}$ values in Table 2 are calculated for the entire duplex; therefore, the changes for duplexes with TAMS or internal loops include PEG effects on the Watson–Crick pairs also. Thus, the TAMS are most sensitive to the effects of PEG 200. The TAMS may have different base stacking, structures, and dynamics that have different water hydration than internal loops.

Table 3 compares the effects of different molecular weight PEGS at 5% on the stabilities of TAMS and one Watson–Crick pair duplex for individual melting curve fits. The differences in duplex free energies are within experimental error for optical melting experiments. Some higher molecular weight PEG at higher percentages appear to cause aggregation as evidenced by irregular and irreproducible melting curves. Table 4 shows the effects of increasing percentages of PEG 200 and PEG 8000 for a Watson–Crick duplex for individual melting curve fits. Increasing PEG 200 from 0 to 20% decreased the duplex stability from −9.02 to −7.52 kcal/mol. This result is consistent

dx.doi.org/10.1021/jp312154d | J. Phys. Chem. B 2013, 117, 3531–3540

Table 5. Effects of Locked Nucleic Acids on TAMS and Internal Adenosine Loops at 100 mM NaCl

terminal mismatch	ΔG°_{TAMS} [a,c] (kcal/mol) RNA	ΔG°_{TAMS} [a,c] (kcal/mol) LNA adenosines	internal loop	ΔG°_{loop} [b,c] (kcal/mol) RNA	ΔG°_{loop} [b,c] (kcal/mol) LNA adenosines	$\Delta\Delta G^{\circ d}$ (kcal/mol) RNA	$\Delta\Delta G^{\circ d}$ (kcal/mol) LNA adenosines
5′**AAA**GCGC**AAA**	−1.6	−2.3	5′CGC**AAA**GCG	+3.8[c]	−1.3	+5.4	+1.0
5′**AA**GCGC**AA**	−1.4	−1.9	5′CGC**AA**GCG	+1.9	−1.6	+3.3	+0.4
5′**A**GCGC**A**	−1.4	−1.5	5′CGC**A**GCG	+1.2	−0.8	+2.5	+0.7
			average per adenosine:			1.0 ± 0.2	0.2 ± 0.1

[a]The free energy of TAMS is calculated using equation: $\Delta G^\circ_{TAMS} = (\Delta G^\circ_{duplex\ with\ TAMS} - \Delta G^\circ_{stem\ helix})/2$. Note that the duplexes with TAMS are self-complementary and have a TAMS motif at each end. [b]The free energy of internal loops is calculated using equation: $\Delta G^\circ_{loop} = \Delta G^\circ_{duplex\ with\ loop} - (\Delta G^\circ_{stem\ helix} - \Delta G^\circ_{NN})$ [c]Calculations use predicted values for the duplex 5′GCGC, the nearest neighbor 5′CG/3′GC, and 5′CGCAAAGCG in 100 mM NaCl, which are too unstable to measure with optical melting experiments, using equation: [d]$\Delta\Delta G^\circ$ is the difference between the ΔG°_{loop} and ΔG°_{TAMS} values. The average per adenosine value is the average of the $\Delta\Delta G^\circ$ values each divided by the number of adenosines in the loop or TAMS.

with previous measurements of a nonself-complementary RNA duplex.[41] Increasing PEG 8000 from 0 to 20% decreased the duplex stability from −8.73 to −7.68 kcal/mol. The net change in duplex stability for PEG 200 and PEG 8000 appears to be similar within experimental error for individual melt curves. However, the different sizes, fraction exposed surface area, excluded volume and thus the ability to interact and stabilize nucleotides or ability to act as a crowding reagent are very different for PEG 200 and PEG 8000. Thus, a different balance of interactions may explain the same net change in stabilities in PEG 200 and PEG 8000. More detailed studies would be necessary to parse the contributions from different molecular interactions in each case. The small size of PEG 200 is better able to disrupt the ions and waters around RNA and DNA duplexes than larger PEGs such as PEG 8000. The small size of PEG 200 also facilitates preferential interactions with RNA bases in the single strand.[42] The data in Tables 3 and 4 provide a few reference points for comparison of the effects of PEG 200 on TAMS in RNA duplexes.

PEG 200 has a destabilizing effect on TAMS, which is consistent with adenosine stacking in an A-form conformation and unlike the stabilizing effect of PEG 200 on Hoogsteen pairs in DNA.[47] The destabilizing effect of PEG 200 on TAMS is larger than the PEG 200 effects for RNA duplexes or internal loops. This result suggests that the adenosine stacking interactions may not be exactly the same in TAMS, internal loops, and Watson−Crick duplexes. Thus, the adenosine stacking interactions may change when comparing terminal mismatches and internal loops and make an enthalpic contribution to the penalty for closing an internal loop, although the magnitude of this enthalpic effect appears to be much smaller than the entropic effects of LNA substitutions.

The Stabilizing Effects of LNA Substitutions Are Larger for Internal Loops than for TAMS. LNA substitutions dramatically stabilize internal loops and only slightly stabilize TAMS. The last column in Table 2 shows the comparison of the duplex free energies in 100 mM NaCl with and without LNA substitutions for all of the adenosines in the loops. The average additional stability per LNA substitution is −1.8 and −0.2 kcal/mol for internal loops and TAMS, respectively. The additional stability of an LNA substitution in a Watson−Crick RNA duplex is 4 °C per substitution.[75] The increase in melting temperatures for an LNA substitution in terminal loops is less than 4 °C but larger in internal loops (Supporting Information Table S2). Although the change in heat capacity for DNA duplexes with LNA is nonzero,[65,67] the average change in heat capacity is 42 cal/mol·K, which is small and within experimental error of the enthalpy measurement in optical melting experiments. Thus, heat capacity changes are not likely to affect the measured free energies of short oligomers with LNA substitutions.

Table 5 shows the calculated free energies of TAMS and internal loop formation with and without LNA substitutions. The free energy of TAMS and internal mismatches are calculated by the following equations:

$$\Delta G^\circ_{TAMS} = (\Delta G^\circ_{duplex\ with\ TAM} - \Delta G^\circ_{stem\ helix})/2 \quad (3)$$

$$\Delta G^\circ_{internal\ loop} = \Delta G^\circ_{duplex\ with\ loop} - (\Delta G^\circ_{stem\ helix} - \Delta G^\circ_{NN}) \quad (4)$$

ΔG°_{NN} is the nearest neighbor term in the INN-HB model for predicting RNA duplex stabilities.[73] The free energy of internal loop formation is unfavorable in regular RNA but is favorable with LNA substitutions. The 3 × 3 internal loop is too unstable to observe in optical melting experiments in less than 1 M NaCl, but forms a stable duplex with LNA substitutions in 100 mM NaCl. Equation 2 allows for prediction of the free energy of loops, short duplexes, and nearest neighbors that cannot be directly measured in an optical melting experiment. The $\Delta\Delta G^\circ$ value is a comparison between the internal loops and terminal mismatches free energy and provides an estimate of the energetic cost of closing an internal loop. The average difference in loop free energies between internal loops and terminal mismatches in 1 M NaCl is 4.7 ± 0.3 kcal/mol.[6] The average difference in loop free energies in 100 mM NaCl is consistent with eq 2. The free energy difference between internal loops and TAMS with LNA substitutions is less than 1 kcal/mol, which suggests only small conformational changes between the two motifs and a small cost of closing the internal loop. The per nucleotide average difference in free energies between internal loops and terminal mismatches is 1.0 ± 0.2 kcal/mol and 0.2 ± 0.2 kcal/mol for loops with RNA and LNA substitutions, respectively. This result demonstrates that the energetic cost of closing an RNA internal loop is largely an entropic effect.

Adenosines in single stranded oligomers sample stacked conformations, and LNA substitutions stabilize these stacking interactions in a preorganization effect demonstrated by NMR of short single strand fragments with LNA substitutions.[50] Thus, adenosines with LNA sugars can stack well in both the single strand and duplex conformations. If the stacking interactions are similar in both the single strand and duplex conformations, then little additional stability will be measured in an optical melting experiment, which is the case for the free energy of TAMS with LNA. A much larger change in free energy and stability occurs with LNA substitutions in internal

dx.doi.org/10.1021/jp312154d | J. Phys. Chem. B 2013, 117, 3531−3540

loops. This result is consistent with previous measurements of single LNA substitutions in 2′Omethyl oligomers that note a larger effect on single internal mismatches than single terminal mismatches.[76] Although the free energy difference for an internal loop with or without LNA is large, the free energy of forming TAMS with LNA or an internal loop with LNA is similar. This suggests similar LNA adenosine stacking in the single strand, internal loop, and terminal mismatch. In regular RNA, the unfavorable stability of internal loops and the favorable stability of terminal mismatches, suggests that the adenosines have different stacking conformations and dynamics in single strands, internal loops, and terminal mismatches. Although adenosines in RNA symmetric internal loops stack and hydrogen bond,[77] significant nucleotide dynamics also contribute to the loop structure and stability as evidenced by the large change in free energy when conformational flexibility is reduced by LNA substitutions.

The experimental measurement of the effects of LNA substitutions on terminal mismatches and internal loops provides insight into the fundamental physical basis for the loop initiation term used to predict RNA thermodynamic stabilities. The similarities in stabilities for terminal mismatches and internal loops with LNA substitutions contrast with the large change in free energies between terminal mismatches and internal loops in RNA. This disparity reveals that the free energy penalty for RNA internal loop formation is largely entropic and experimentally confirms theoretical models.[78] The similar stability of terminal and internal loops with LNA substitutions suggests no apparent changes in stacking or hydrogen bonding. Thus internal loop closure does not necessarily prevent the most favorable stacking interactions, and changes in stacking and enthalpy are not necessarily a primary contribution to the penalty for RNA loop formation. Because the trends in salt effects in regular RNA are similar for terminal mismatches, internal loops, and Watson−Crick duplexes, the entropic cost of RNA internal loop formation is not likely due to changes in ions and water activities. Thus, the entropic penalty for loop formation may be due to conformational dynamics in the RNA backbone and base stacking and the restriction of these dynamics by forming an internal loop.

CONCLUSIONS

These measurements of TAMS, internal loops, and Watson−Crick duplexes with different salt conditions, LNA substitution, and PEG conditions provide benchmarks for predicting the stabilities of RNA oligomers in physiological or therapeutic conditions. The unified prediction rule for the salt effects will be a useful tool for estimating RNA duplex stabilities for therapeutic applications. The salt dependence is similar for RNA duplexes with TAMS, internal loops, and only Watson−Crick pairs as well as DNA duplexes (eq 2). This result validates the simplifying assumptions of polyelectrolyte theories. The effects of LNA substitutions and PEG effects suggest that adenosines stack in terminal mismatches, which is important for the thermodynamic stability of miRNA-mRNA duplexes and molecular recognition of these imperfect RNA duplexes by proteins such as argonaute. The large effect of LNA substitutions on the comparisons of terminal mismatch and internal loop stabilities suggests that the energetic cost of closing an RNA internal loop is largely entropic. Although the PEG effects suggest some difference in adenosine stacking interactions between terminal mismatches and internal loops, these enthalpic contributions to the energetic penalty for internal loop formation are much less than the entropic contributions observed from LNA substitutions.

ASSOCIATED CONTENT

Supporting Information

A table of the complete data set of salt dependence for thermodynamic parameters and a table comparing T_m changes for LNA substitutions. This material is available free of charge via the Internet at http://pubs.acs.org.

AUTHOR INFORMATION

Corresponding Author

*Phone: (405) 325-3092; fax: (405) 325-6111; e-mail: susan.schroeder@ou.edu.

Notes

The authors declare no competing financial interest.

ACKNOWLEDGMENTS

This work was supported by the Oklahoma Center for the Advancement of Science and Technology grant HR09−160 and a National Science Foundation CAREER Grant No. 0844913.

ABBREVIATIONS

TAMS, Terminal adenosine mismatches; LNA, locked nucleic acid; PEG, polyethylene glycol

REFERENCES

(1) Kozomara, A.; Griffiths-Jones, S. miRBase: Integrating microRNA Annotation and Deep-Sequencing Data. *Nucleic Acids Res.* **2011**, *39*, D152−7.

(2) Doench, J. G.; Sharp, P. A. Specificity of microRNA Target Selection in Translational Repression. *Genes Dev.* **2004**, *18*, 504−511.

(3) Zamore, P.; Tuschl, D.; Sharp, T.; Bartel, P. A.; RNAi, D. A.; Double-Stranded, R. N. A. Directs the ATP-Dependent Cleavage of mRNA at 21 to 23 Nucleotide Intervals. *Cell* **2000**, *101*, 25−33.

(4) Haley, B.; Zamore, P. D. Kinetic Analysis of the RNAi Enzyme Complex. *Nat. Struct. Biol.* **2004**, *11*, 599−606.

(5) Ameres, S. L.; Martinez, J.; Schroeder, R. Molecular Basis for Target RNA Recognition and Cleavage by Human RISC. *Cell* **2007**, *130*, 101−112.

(6) Clanton-Arrowood, K.; McGurk, J.; Schroeder, S. J. 3′ Terminal Nucleotides Determine Thermodynamic Stabilities of Mismatches at the Ends of RNA Helices. *Biochemistry* **2008**, *47*, 13418−13427.

(7) Ohmichi, T.; Nakano, S.; Miyoshi, D.; Sugimoto, N. Long Dangling End Has Large Energetic Contribution to Duplex Stability. *J. Am. Chem. Soc.* **2002**, *124*, 10367−10372.

(8) O'Toole, A. S.; Miller, S.; Haines, N.; Zink, M. C.; Serra, M. J. Comprehensive Thermodynamic Analysis of 3′ Double Nucleotide Overhangs Neighboring Watson-Crick Terminal Base Pairs. *Nucleic Acids Res.* **2006**, *34*, 3338−3344.

(9) Lewis, B. P.; Burge, C. B.; Bartel, D. P. Conserved Seed Pairing, Often Flanked by Adenosines, Indicates That Thousands of Human Genes are microRNA Targets. *Cell* **2005**, *120*, 15−20.

(10) Manning, G. S. The Molecular Theory of Polyelectrolyte Solutions with Applications to the Electrostatic Properties of Polynucleotides. *Q. Rev. Biophys.* **1978**, *11*, 179−246.

(11) Bloomfield, V. A., Crothers, D. M., Tinoco, I., Jr., Interactions of Nucleic Acids and Water and Ions. In *Nucleic Acids Structures, Properties, and Functions*; University Science Books: Sausalito, CA, 2000; pp 475−534.

(12) Holmstrom, E. D.; Fiore, J. L.; Nesbitt, D. J. Thermodynamic Origins of Monovalent Facilitated RNA Folding. *Biochemistry* **2012**, *51*, 3732−3743.

(13) Fiore, J. L.; Holmstrom, E. D.; Nesbitt, D. J. Entropic Origin of Mg^{2+}-Facilitated RNA Folding. *Proc. Natl. Acad. Sci. U.S.A.* **2012**, *109*, 2902−2907.

(14) Leipply, D.; Lambert, D.; Draper, D. E. Ion−RNA Interactions Thermodynamic Analysis of the Effects of Mono- And Divalent Ions on RNA Conformational Equilibria. *Methods Enzymol.* **2009**, *469*, 433−463.
(15) Moghaddam, S.; Caliskan, G.; Chauhan, S.; Hyeon, C.; Briber, R. M.; Thirumalai, D.; Woodson, S. A. Metal Ion Dependence of Cooperative Collapse Transitions in RNA. *J. Mol. Biol.* **2009**, *393*, 753−764.
(16) Kieft, J. S.; Chase, E.; Costantino, D. A.; Golden, B. L. Identification and Characterization of Anion Binding Sites in RNA. *RNA* **2010**, *16*, 1118−1123.
(17) Keel, A.; Rambo, R.; Batey, R.; Kieft, J. A General Strategy to Solve the Phase Problem in RNA Crystallography. *Structure* **2007**, *15*, 761−772.
(18) Kieft, J. S.; Tinoco, I., Jr. Solution Structure of a Metal-Binding Site in the Major Groove of RNA Complexed with Cobalt (III) Hexammine. *Structure* **1997**, *5*, 713−721.
(19) Tan, Z. J.; Chen, S. J. Salt Contribution to RNA Tertiary Structure Folding Stability. *Biophys. J.* **2011**, *101*, 176−187.
(20) Koculi, E.; Hyeon, C.; Thirumalai, D.; Woodson, S. A. Charge Density of Divalent Metal Cations Determines RNA Stability. *J. Am. Chem. Soc.* **2007**, *129*, 2676−2682.
(21) Freier, S. M.; Petersheim, M.; Hickey, D. R.; Turner, D. H. Thermodynamic Studies of RNA Stability. *J. Biomol. Struct. Dyn.* **1984**, *1*, 1229−1242.
(22) Nakano, S.; Fujimoto, M.; Hara, H.; Sugimoto, N. Nucleic Acid Duplex Stability: Influence of Base Composition on Cation Effects. *Nucleic Acids Res.* **1999**, *27*, 2957−2965.
(23) Serra, M.; Baird, J. D.; Dale, Taraka, D.; Fey, B. L.; Retatagos, K.; Westof, E. Effects of Magnesium Ions on the Stabilization of RNA Oligomers of Defined Structures. *RNA* **2002**, *8*, 307−323.
(24) SantaLucia, J., Jr. A Unified View of Polymer, Dumbbell, And Oligonucleotide DNA Nearest-Neighbor Thermodynamics. *Proc. Natl. Acad. Sci. U.S.A.* **1998**, *95*, 1460−1465.
(25) Williams, D. J.; Hall, K. B. Thermodynamic Comparison of the Salt Dependence of Natural RNA Hairpins and RNA Hairpins with Non-Nucleotide Spacers. *Biochemistry* **1996**, *35*, 14665−14670.
(26) Owczarzy, R.; You, Y.; Moreira, B. G.; Manthey, J. A.; Huang, L.; Behlke, M. A.; Walder, J. A. Effects of Sodium Ions on DNA Duplex Oligomers: Improved Predictions of Melting Temperatures. *Biochemistry* **2004**, *43*, 3537−3554.
(27) Williams, A.; Longfellow, C.; Freier, S.; Kierzek, R.; Turner, D. Laser Temperature-Jump, Spectroscopic, And Thermodynamic Study of Salt Effects on Duplex Formation by dGCATGC. *Biochemistry* **1989**, *28*, 4283−4291.
(28) Record, M. T., Jr.; Lohman, T. M. A Semiempirical Extension of Polyelectrolyte Theory to the Treatment of Oligoelectrolytes: Application to Oligonucleotide Helix-Coil Transitions. *Biopolymers* **1978**, *17*, 159−166.
(29) Olmsted, M. C.; Anderson, C. F.; Record, M. T., Jr. Importance of Oligoelectrolyte End Effects for the Thermodynamics of Conformational Transitions of Nucleic Acid Oligomers: A Grand Canonical Monte Carlo Analysis. *Biopolymers* **1991**, *31*, 1593−1604.
(30) Blose, J. M.; Proctor, D. J.; Veeraraghavan, N.; Misra, V. K.; Bevilacqua, P. C. Contribution of the Closing Base Pair to Exceptional Stability in RNA Tetraloops: Roles for Molecular Mimicry and Electrostatic Factors. *J. Am. Chem. Soc.* **2009**, *131*, 8474−8484.
(31) Vieregg, J.; Cheng, W.; Bustamante, C.; Tinoco, I., Jr. Measurement of the Effect of Monovalent Cations on RNA Hairpin Stability. *J. Am. Chem. Soc.* **2007**, *129*, 14966−14973.
(32) Lambert, D.; Draper, D. E. Effects of Osmolytes on RNA Secondary and Tertiary Structure Stabilities and RNA-Mg^{2+} Interactions. *J. Mol. Biol.* **2007**, *370*, 993−1005.
(33) Kilburn, D.; Roh, J. H.; Guo, L.; Briber, R. M.; Woodson, S. A. Molecular Crowding Stabilizes Folded RNA Structure by the Excluded Volume Effect. *J. Am. Chem. Soc.* **2010**, *132*, 8690−8696.
(34) Nakano, S.; Karimata, H. T.; Kitagawa, Y.; Sugimoto, N. Facilitation of RNA Enzyme Activity in the Molecular Crowding Media of Cosolutes. *J. Am. Chem. Soc.* **2009**, *131*, 16881−16888.
(35) Nakano, S. I.; Hirayama, H.; Miyoshi, D.; Sugimoto, N. Dimerization of Nucleic Acid Hairpins in the Conditions Caused by Neutral Cosolutes. *J. Phys. Chem. B* **2012**, *116* (25), 7406−7415.
(36) Denesyuk, N. A.; Thirumalai, D. Crowding Promotes the Switch from Hairpin to Pseudoknot Conformation in Human Telomerase RNA. *J. Am. Chem. Soc.* **2011**, *133*, 11858−11861.
(37) Yu, H. Q.; Zhang, D. H.; Gu, X. B.; Miyoshi, D.; Sugimoto, N. Regulation of Telomerase Activity by the Thermodynamic Stability of a DNA × RNA Hybrid. *Angew. Chem.* **2008**, *47*, 9034−9038.
(38) Yu, H.; Gu, X.; Nakano, S. I.; Miyoshi, D.; Sugimoto, N. Beads-on-a-String Structure of Long Telomeric DNAs under Molecular Crowding Conditions. *J. Am. Chem. Soc.* **2012**, *134* (49), 20060−20069.
(39) Zhang, D.-H.; Fujimoto, T.; Saxena, Yu, H.-Q.; Miyoshi, D.; Sugimoto, N. Monomorphic RNA G-Quadruplex and Polymorphic DNA G-Quadruplex Structures Responding to Cellular Environmental Factors. *Biochemistry* **2010**, *49*, 4554−4563.
(40) Muhuri, S.; Mimura, K.; Miyoshi, D.; Sugimoto, N. Stabilization of Three-Way Junctions of DNA under Molecular Crowding Conditions. *J. Am. Chem. Soc.* **2009**, *131*, 9268−9280.
(41) Pramanik, S.; Nagatoishi, S.; Saxena, S.; Bhattacharyya, J.; Sugimoto, N. Conformational Flexibility Influences Degree of Hydration of Nucleic Acid Hybrids. *J. Phys. Chem. B* **2011**, *115*, 13862−13872.
(42) Knowles, D. B.; LaCroix, A. S.; Deines, N. F.; Shkel, I.; Record, M. T., Jr. Separation of Preferential Interaction and Excluded Volume Effects on DNA Duplex and Hairpin Stability. *Proc. Natl. Acad. Sci. U.S.A.* **2011**, *108*, 12699−12704.
(43) Nakano, S.; Wu, L.; Oka, H.; Karimata, H. T.; Kirihata, T.; Sato, Y.; Fujii, S.; Sakai, H.; Kuwahara, M.; Sawai, H.; et al. Conformation and the Sodium Ion Condensation on DNA and RNA Structures in the Presence of a Neutral Cosolute As a Mimic of the Intracellular Media. *Mol. BioSyst.* **2008**, *4*, 579−588.
(44) Nakano, S.; Karimata, H.; Ohmichi, T.; Kawakami, J.; Sugimoto, N. The Effect of Molecular Crowding with Nucleotide Length and Cosolute Structure on DNA Duplex Stability. *J. Am. Chem. Soc.* **2004**, *126*, 14330−14331.
(45) Gu, X. B.; Nakano, S.; Sugimoto, N. the Effect of the Structure of Cosolutes on the DNA Duplex Formation. *Nucl. Acids Symp. Ser.* **2006**, 205−206.
(46) Gu, X. B.; Nakano, S.; Sugimoto, N. Consecutive GC Base Pairs Determine the Energy Barrier of DNA Duplex Formation under Molecularly Crowded Conditions. *Chem. Commun.* **2007**, 2750−2752.
(47) Miyoshi, D.; Nakamura, K.; Tateishi-Karimata, H.; Ohmichi, T.; Sugimoto, N. Hydration of Watson-Crick Base Pairs and Dehydration of Hoogsteen Base Pairs Inducing Structural Polymorphism under Molecular Crowding Conditions. *J. Am. Chem. Soc.* **2009**, *131*, 3522−35231.
(48) Kumar, R.; Singh, S. K.; Koshkin, A. A.; Rajwanshi, V. K.; Meldgaard, M.; Wengel, J. The First Analogues of LNA (Locked Nucleic Acids): Phosphorothioate-LNA and 2′-thio-LNA. *Bioorg. Med. Chem. Lett.* **1998**, *8*, 2219−2222.
(49) Petersen, M.; Bondensgaard, K.; Wengel, J.; Jacobsen, J. P. Locked Nucleic Acid (LNA) Recognition of RNA: NMR Solution Structures of LNA:RNA Hybrids. *J. Am. Chem. Soc.* **2002**, *124*, 5974−5982.
(50) Kierzek, E.; Pasternak, A.; Pasternak, K.; Gdaniec, Z.; Yildirim, I.; Turner, D. H.; Kierzek, R. Contributions of Stacking, Preorganization, And Hydrogen Bonding to the Thermodynamic Stability of Duplexes between RNA and 2′-O-methyl RNA with Locked Nucleic Acids. *Biochemistry* **2009**, *48*, 4377−4387.
(51) Elmen, J.; Lindow, M.; Schutz, S.; Lawrence, M.; Petri, A.; Obad, S.; Lindholm, M.; Hedtjarn, M.; Hansen, H. F.; Berger, U.; et al. LNA-Mediated microRNA Silencing in Non-Human Primates. *Nature* **2008**, *452*, 896−899.
(52) Laxton, C.; Brady, K.; Moschos, S.; Turnpenny, P.; Rawal, J.; Pryde, D. C.; Sidders, B.; Corbau, R.; Pickford, C.; Murray, E. J. Selection, Optimization, And Pharmacokinetic Properties of a Novel, Potent Antiviral Locked Nucleic Acid-Based Antisense Oligomer

Targeting Hepatitis C Virus Internal Ribosome Entry Site. *Antimicrob. Agents Chemother.* **2011**, *55*, 3105−3114.
(53) Fabani, M. M.; Gait, M. J. miR-122 targeting with LNA/2′-O-Methyl Oligonucleotide Mixmers, Peptide Nucleic Acids (PNA), and PNA-Peptide Conjugates. *RNA* **2008**, *14*, 336−346.
(54) Childs, J. L.; Disney, M. D.; Turner, D. H. Oligonucleotide Directed Misfolding of RNA Inhibits *Candida albicans* Group I Intron Splicing. *Proc. Natl. Acad. Sci. U.S.A.* **2002**, *99*, 11091−11096.
(55) Fluiter, K.; Frieden, M.; Vreijling, J.; Rosenbohm, C.; De Wissel, M. B.; Christensen, S. M.; Koch, T.; Orum, H.; Baas, F. on the in Vitro and in Vivo Properties of Four Locked Nucleic Acid Nucleotides Incorporated into an anti-H-Ras Antisense Oligonucleotide. *Chembiochem: Eur. J. Chem. Biol.* **2005**, *6*, 1104−1109.
(56) Wahlestedt, C.; Salmi, P.; Good, L.; Kela, J.; Johnsson, T.; Hokfelt, T.; Broberger, C.; Porreca, F.; Lai, J.; Ren, K.; et al. Potent and Nontoxic Antisense Oligonucleotides Containing Locked Nucleic Acids. *Proc. Natl. Acad. Sci. U.S.A.* **2000**, *97*, 5633−5638.
(57) Vester, B.; Wengel, J. LNA (Locked Nucleic Acid): High-Affinity Targeting of Complementary RNA and DNA. *Biochemistry* **2004**, *43*, 13233−13241.
(58) Mook, O. R.; Baas, F.; de Wissel, M. B.; Fluiter, K. Evaluation of Locked Nucleic Acid-Modified Small Interfering RNA in Vitro and in Vivo. *Mol. Cancer Ther.* **2007**, *6*, 833−843.
(59) Fluiter, K.; Mook, O. R.; Baas, F. The Therapeutic Potential of LNA-Modified siRNAs: Reduction of off-Target Effects by Chemical Modification of the siRNA Sequence. *Methods Mol. Biol.* **2009**, *487*, 189−203.
(60) Campbell, M. A.; Wengel, J. Locked vs. Unlocked Nucleic Acids (LNA vs. UNA): Contrasting Structures Work Towards Common Therapeutic Goals. *Chem. Soc. Rev.* **2011**, *40*, 5680−5689.
(61) Kierzek, E.; Ciesielska, A.; Pasternak, K.; Mathews, D. H.; Turner, D. H.; Kierzek, R. The Influence of Locked Nucleic Acid Residues on the Thermodynamic Properties of 2′-O-Methyl RNA/RNA Heteroduplexes. *Nucl. Acids Res.* **2005**, *33*, 5082−5093.
(62) Owczarzy, R.; You, Y.; Groth, C. L.; Tataurov, A. V. Stability and Mismatch Discrimination of Locked Nucleic Acid-DNA Duplexes. *Biochemistry* **2011**, *50*, 9352−9367.
(63) You, Y.; Moreira, B. G.; Behlke, M. A.; Owczarzy, R. Design of LNA Probes That Improve Mismatch Discrimination. *Nucl. Acids Res.* **2006**, *34*, e60.
(64) McTigue, P. M.; Peterson, R. J.; Kahn, J. D. Sequence-Dependent Thermodynamic Parameters for Locked Nucleic Acid (LNA)−DNA Duplex Formation. *Biochemistry* **2004**, *43*, 5388−5405.
(65) Hughesman, C. B.; Turner, R. F.; Haynes, C. A. Role of the Heat Capacity Change in Understanding and Modeling Melting Thermodynamics of Complementary Duplexes Containing Standard and Nucleobase-Modified LNA. *Biochemistry* **2011**, *50*, 5354−5368.
(66) Kaur, H.; Arora, A.; Wengel, J.; Maiti, S. Thermodynamic, Counterion, And Hydration Effects for the Incorporation of Locked Nucleic Acid Nucleotides into DNA duplexes. *Biochemistry* **2006**, *45*, 7347−7355.
(67) Kaur, H.; Wengel, J.; Maiti, S. Thermodynamics of DNA−RNA Heteroduplex Formation: Effects of Locked Nucleic Acid Nucleotides Incorporated into the DNA strand. *Biochemistry* **2008**, *47*, 1218−1227.
(68) Peritz, A.; Kierzek, Sugimoto, N.; Turner, D. H. Thermodynamic Study of Internal Loops in Oligoribonucleotides: Symmetric Loops Are More Stable than Asymmetric Loops. *Biochemistry* **1991**, *30*, 6428−6436.
(69) Borer, P. N. *Handbook of Biochemistry and Molecular Biology: Nucleic Acids*, 3rd ed.; CRC Press: Cleveland, OH, 1975; Vol. *1*, p 589.
(70) Petersheim, M.; Turner, D. H. Base-Stacking and Base-Pairing Contributions to Helix Stability: Thermodynamics of Double-Helix Formation with CCGG, CCGGp, CCGGAp, ACCGGp, CCGGUp, and ACCGGUp. *Biochemistry* **1983**, *22*, 256−263.
(71) McDowell, J. A.; Turner, D. H. Investigation of the Structural Basis for Thermodynamic Stabilities of Tandem GU Mismatches: Solution Structure of (rGAGGUCUC)2 by Two-Dimensional NMR and Simulated Annealing. *Biochemistry* **1996**, *35*, 14077−14089.
(72) Borer, P. D.; B., Tinoco, I., Jr.; Uhlenbeck, O. C. Stability of Ribonucleic Double-Stranded Helices. *J. Mol. Biol.* **1974**, *86*, 843−853.
(73) Xia, T.; Santa Lucia, J., Jr.; Burkard, M. E.; Kierzek, R.; Schroeder, S. J.; Jiao, X.; Cox, C.; Turner, D. H. Thermodynamic Parameters for an Expanded Nearest-Neighbor Model for Formation of RNA Duplexes with Watson-Crick Base Pairs. *Biochemistry* **1998**, *37*, 14719−14735.
(74) Nguyen, M.-T.; Schroeder, S. J. Consecutive Terminal GU Pairs Stabilize RNA Helices. *Biochemistry* **2010**, *49*, 10574−10581.
(75) Singh, S. K.; Wengel, J. Universality of LNA-Mediated High-Affinity Nucleic Acid Recognition. *Chem. Commun.* **1998**, 1247−1248.
(76) Kierzek, E.; Ciesielska, A.; Pasternak, K.; Mathews, D. H.; Turner, D. H.; Kierzek, R. The Influence of Locked Nucleic Acid Residues on the Thermodynamic Properties of 2′-O-methyl RNA/RNA Heteroduplexes. *Nucl. Acids Res.* **2005**, *33*, 5082−5093.
(77) Znosko, B. M.; Burkard, M. E.; Schroeder, S. J.; Krugh, T. R.; Turner, D. H. Sheared Aanti.Aanti Base Pairs in a Destabilizing 2 × 2 Internal Loop: The NMR Structure of 5′(rGGCAAGCCU)2. *Biochemistry* **2002**, *41*, 14969−14977.
(78) Turner, D. H. Conformational Changes. In *Nucleic Acids: Structures, Properties, and Functions*; Bloomfield, V. A., Crothers, D. M., Tinoco, I., Jr., Eds.; University Science Books: Sausalito, CA, 2000; pp 259−334.